International Journal of Mechanical, Industrial and Aerospace Sciences
ISSN: 2517-9950
Vol:11, No:5, 2017

Low Power Consuming Electromagnetic Actuators for Pulsed Pilot Stages

M. Honarpardaz, Z. Zhang, J. Derkx, A. Trangärd, J. Larsson

***Abstract*—**Pilot stages are one of the most common positioners and regulators in industry. In this paper, we present two novel concepts for pilot stages with low power consumption to regulate a pneumatic device. Pilot 1, first concept, is designed based on a conventional frame core electro-magnetic actuator and a leaf spring to control the air flow and pilot 2 has an axisymmetric actuator and spring made of non-oriented electrical steel. Concepts are simulated in a system modeling tool to study their dynamic behavior. Both concepts are prototyped and tested. Experimental results are comprehensively analyzed and compared. The most promising concept that consumes less than 8 mW is highlighted and presented.

***Keywords*—**Electro-magnetic actuator, multidisciplinary system, low power consumption, pilot stage.

I. Introduction

PILOT stages are widely used in industrial systems. Usually, these devices are utilized to translate a (small) electrical signal into a pneumatic output. A common type of pilot stages is pulsed pilot which is based on a very simple on-off valve. These valves have two states: close and open. To control the flow of such a simple (discrete) valve system, the switching of the valve needs to be controlled in a very dynamic way. In practice, the flapper-nozzle pilot valve is a typical structure of the pilot stage, which is used extensively due to its high dynamic response in comparison with other types of pilot valves [1]-[4]. The most common way to realize this is by switching the valve with a base frequency and varying the relative open time within a cycle. This is called a pulse width modulation (PWM). The pilots use pneumatic micro-valves of the on/off type that are being driven in a pneumatically PWM controlled mode. Other control schemes would be possible, but are not further explored in this work.

Existing pilot stages (I/p converter) work in an analog way where a flapper is positioned closely to a nozzle that creates a very small gap, to restrict the flow. Thus, position of the flapper is changed to achieve a different flow/pressure.

A pulsed pilot stage would have the advantage that it does not need any adjustment of the two defined states of open or close. Furthermore, an on-off valve would have the potential to be manufactured in a very cost efficient way. Several numerical studies on flapper-nozzle have been performed [5], [6].

In order to achieve a low power consuming pulsed pilot stage, selecting a proper actuator is essential. Actuators are utilized to convert a certain kind of energy into mechanical energy. There are different types of actuators, depending on the physical principle behind these actuators, such as hydraulic actuators, electrostatic actuators, electromagnetic actuators, thermal expansion actuators, pneumatic actuators and even linear piezoelectric motor [7]. All of these actuators are widely used in industrial applications.

Electromagnetic actuator is currently used in a broad range of applications, such as electrical motors, relays, circuit breakers, etc. There are many novel designs with new topologies, like linear actuator in [8], planar motor in [9], rotary-linear actuator studied in [10], and ball-joint-like spherical actuator [11]. All these actuators were designed to meet performance specifications with mechanically simple structures.

In some specific applications, actuator is required to be low energy consumption. In reference [12], a low energy actuator for driving microfluidic valves in biomedical applications is introduced. Another common low energy actuator is microelectromechanical systems (MEMs). In the last decades, MEMs technology has various designs and applications [13]-[15]. Meanwhile, this technology has not been introduced to the actuators market yet and is still in the stage of research and development in labs.

The use of a pulsed valve to control a flow in general is not new. However, an application as a pilot stage for a positioner, to control a proportional main stage valve, is not known to the author. Therefore, efforts in this study have been towards the development of a pilot valve that can be switched at a 100-Hz base frequency, in PWM controlled mode, and at a maximum power consumption of 8 mW. The input pressure of the nozzle is 10 bar, and the minimum force to block the nozzle is 0.14 N. Thus, an electromagnetic actuator is required to be able to execute enough force to displace the spring and open the nozzle.

This paper is divided into sections as follows: the “Relevant Work” section reviews the related works, and the “Method” section describes the utilized methodology. Results are presented and discussed in the “Result” section, and the performance of the conceptual designs are compared and discussed in the “Discussion”.

II. Methods

To design an actuator that regulates the control pressure with PWM technique, the device should have two states:

1. Air flow through the nozzle is blocked (close), when electro-magnetic actuator is inactive.

M. Honarpardaz is with ABB Corporate Research, Västerås, Sweden (phone: +46-738-499-040, e-mail: mohammadali.honarpardaz@ se.abb.com).
Z. Zhang, A. Trangärd and J. Larsson are with ABB Corporate Research, Västerås, Sweden.
J. Derkx is with ABB Robotics, Västerås, Sweden.

2. Full flow through nozzle (open) when electromagnet is active.

Based on the input pressure and dimension of the nozzle, the output flow and minimum force to block the flow are known. Therefore, the actuator should be able to execute enough force to displace the spring and open the nozzle.

Actuators using electromagnets are common in many applications, such as relay, switchgear, etc. A conventional electro-magnetic actuator usually consists of a core of ferromagnetic material (usually laminated iron or steel sheets), a coil of wire wrapped around this iron core, an actuating part (can be a flapper, plunger etc.). Once a current (either AC or DC) flows through the coil, magnetic field is created by this current, and magnetic flux is confined in the core (high permeability), with negligible leakage flux. Within the core, the magnetic field (B) will be approximately uniform across any cross section of the core. There are small air gaps between the core and the actuating part due to the high permeability of the actuating part, thus it moves towards the core until the air gap (or air gaps) becomes zero.

The force exerted by an electromagnet on a section of core material is

$$F = \frac{B^2 A}{2\mu_0} \quad (1)$$

where B is the magnetic flux density, A is the cross-sectional area of the core, μ_0 is the permeability of the air. The force equation can be derived from the energy stored in a magnetic field. Energy is force times distance, re-arranging terms yields the equation above.

In order to get sealing between nozzle and spring, it is essential that the spring is in contact with the nozzle in a perpendicular manner. The spring angle to provide the required force is calculated as:

$$\emptyset = \frac{FL}{2EI} \quad (2)$$

$$I = \frac{b}{12} h^3 \quad (3)$$

where F is the required force to block the nuzzle flow, L is length, E is Young's modulus, and I is the moment of inertia for the section area of the spring.

In order to calculate power consumption of the system, generally, three steps need to be done as follows.

Step1. Obtaining holding power: In order to calculate the holding power consumption, following steps should be considered:

- Setting the spring in the pre-load position to block the nozzle flow.
- Adding an airgap between the flapper and core to allow the full open-state of the nozzle.
- Determine the electro-magnetic force to attract the flapper.
- Obtaining the required current to generate required electro-magnetic force.
- Calculating the power according to (4).

$$P = V.I \quad (4)$$

where V is voltage, and I represents opening current.

Step2. Obtaining minimum and maximum opening power: In order to find out the range of power consumption of the design, the pilot has to be operated once with the minimum performance (just switching) and another time with the 1-ms opening and closing operation time (100 Hz).

Step3. Obtaining total power: In order to find required power, we have to consider the system in 90% duty cycle, which has 10% opening and 80% holding. So, for each situation, we have:

$$P_t = P_o + (0.8)(P_h) \quad (5)$$

where P_t, P_o, and P_h respectively represent total, opening, and holding powers.

As pilot stages are multidisciplinary systems with complex characteristics, analyzing dynamic behavior of the system and calculating power consumption by considering all domains are crucial. However, most of system modeling tools (e.g. Dymola and Simulink) use lumped models to simulate electro-magnetic mechanisms. Therefore, these tools are not accurate enough for calculating complex phenomena such as force exerted by magnetic field. Thus, Finite Element Method (FEM) based models are necessary to calculate more complex and essential variables (i.e. force and inductance).

III. Concept Design

Based on the power consumption constraint and performance requirements, two designs of pulsed pilot stage have been realized which are driven by electro-magnetic actuators.

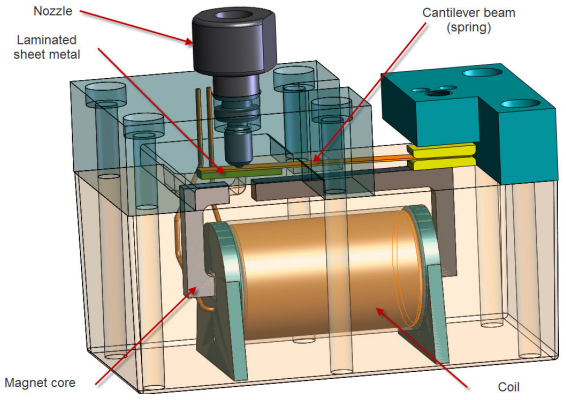

Fig. 1 Conceptual design of pilot 1

A. Pilot 1

This concept consists of a spiral coil, laminated frame core (with seven layers of 0.2 mm sheets), laminated flapper (with two layers of 0.27 mm sheets), cantilever spring and nozzle (see Fig. 1). The core and flapper are made of non-oriented electrical steel with high permeability (NO27 [16]). The basic function of this pilot is to allow the cantilever spring carry the

flapper and control the nozzle pressure. The spring is preloaded against a nozzle. When the coil is energized, magnetic flux flows through the core and attracts the flapper which opens the nozzle flow, as shown in Fig. 2. The nominal gap between the flapper and frame is 0.1 mm. To create a housing for coil and cores, they were put in a mold and casted with epoxy.

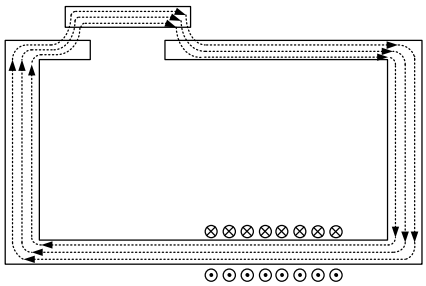

Fig. 2 Magnetic circuit of pilot 1

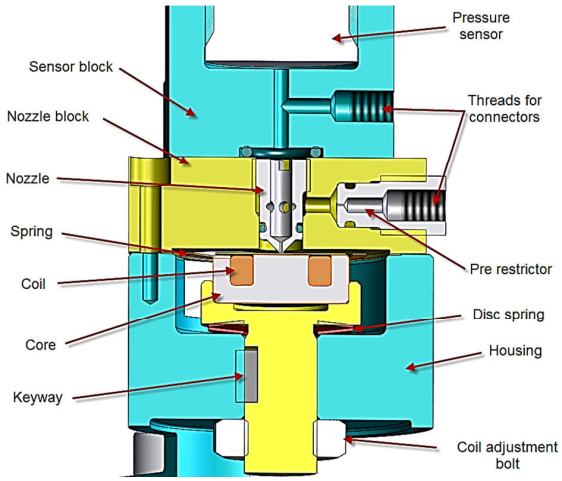

Fig. 3 Conceptual design of pilot 2

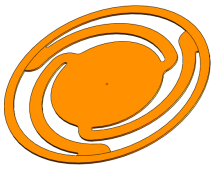

Fig. 4 Spring and flapper of pilot 2

B. Pilot 2

Similar to the pilot 1, a preloaded spring is utilized to control the flow of the nozzle in this concept, as illustrated in Fig. 3. As the moving mass plays a very important role in time constant and power consumption of the system, minimizing this factor is crucial. An effective way to bring down the mass is to reduce the number of moving components. An improvement to pilot 1 could be integrating the spring and magnetic mass in one part. Therefore, in this concept, the spring and flapper are combined together, and both are made from an iron-cobalt-chromium soft magnetic alloy (NO27 [16]), as demonstrated in Fig. 4. In order to be able to fairly compare the results with pilot 1, the moving disc is designed to have the same mass as the flapper in pilot 1. Therefore, thickness of the moving disc is reduced to decrease the total mass. As a consequence, magnetic flux through the disk is also reduced due to the saturation. However, using a coil with an axisymmetric core can counterbalance the reduction of flux and properly concentrate the magnetic flux. In this way, no extra mass (flapper) is required for magnetic attraction since the spring will act as the flapper (see Fig. 4). Besides, this will be beneficial for the mechanical response time of the pilot valve.

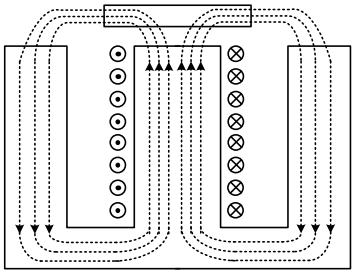

Fig. 5 Magnetic circuit of pilot 2

IV. Results

This section presents the simulation and experimental verification results of conceptual low power consuming pulsed pilot stages.

A. Simulation

To verify feasibility of the conceptual designs, their multi-disciplinary mechanism is modeled in Dymola [17] to investigate the dynamic behavior of the system. As shown in Fig. 6 (a), the model consists of three domains of pneumatics, electro-magnetic and mechanics. The pneumatic domain contains the fluid model of the system which is the air inlet, pipes, and nozzle (see Fig. 6 (b)). The electromagnetic actuator and control mechanism of the system is modeled in the electro-magnetic domain, as illustrated in Fig. 6 (c). In the mechanical domain, the spring and its dynamic interaction with the executed force by the actuator are simulated.

To improve the accuracy of the electro-magnetic domain of the system, the actuator of each pilot is simulated in COMSOL Multi-physics [18], which is a FEM based tool as illustrated in Figs. 7 (a) and (b).

Once inductance, electromagnetic force, resistance and flux density of each concept is determined, results are fed to Dymola in 3D table formats. Two tables are needed for this system. First, a force table containing the electromagnetic force exerted to the flapper as function of flapper position and current (see Fig. 8 (a)). As illustrated in Fig. 8 (b), second table contains the static inductance as function of flapper position and current.

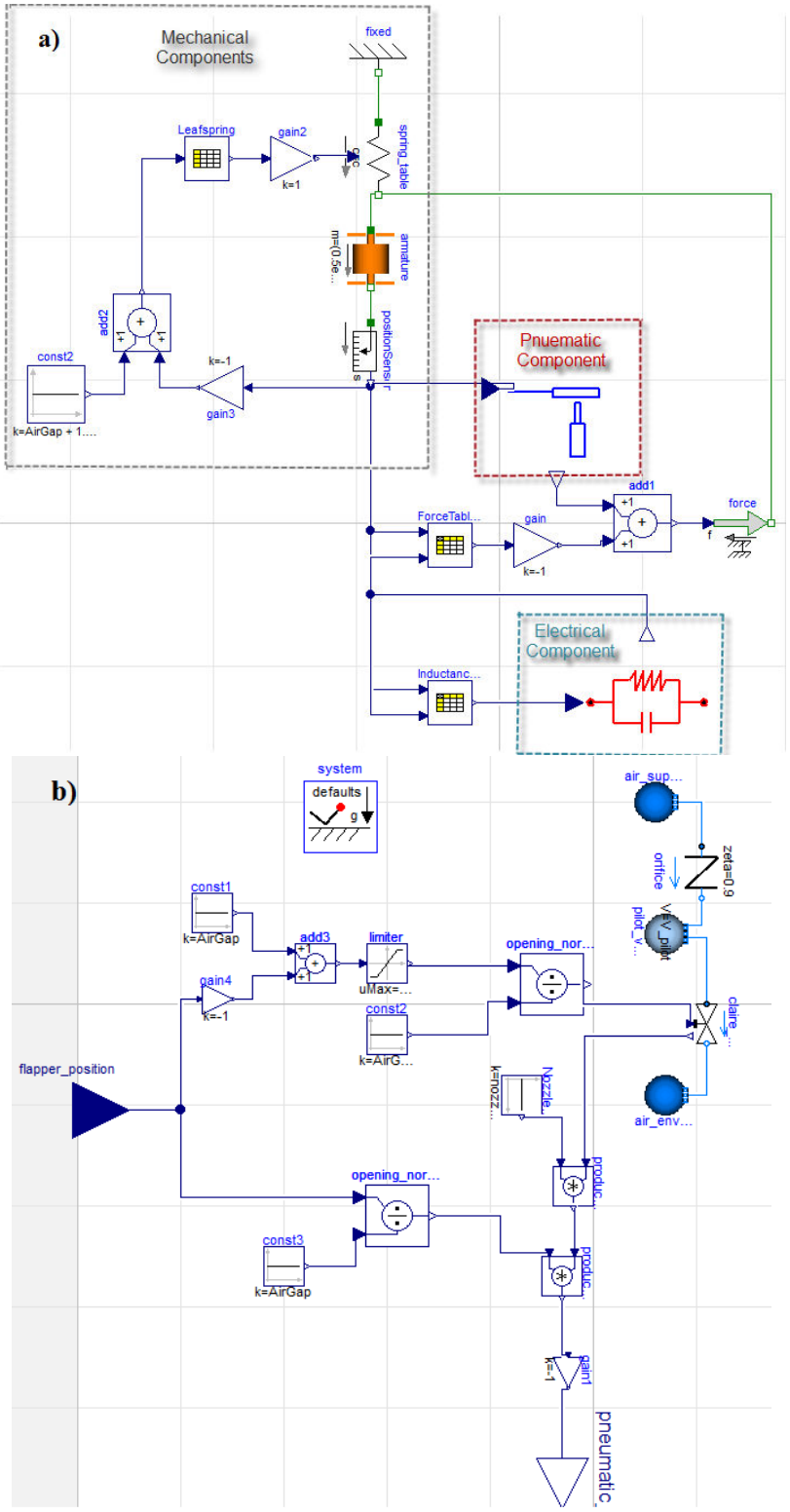
a)
Mechanical Components
fixed
Leafspring
gain2
k=1
spring_table
armature
positionSensor
add2
const2
k=AirGap + 1....
k=-1
gain3
Pnuematic Component
add1
force
ForceTabl...
gain
k=-1
Electrical Component
Inductanc...
b)
system
defaults
g
air_sup...
orifice
zeta=0.9
pilot_v...
const1
k=AirGap
add3
limiter
uMax=...
gain4
k=-1
opening_nor...
const2
k=AirG...
clarre...
flapper_position
Nozzle
k=nozz...
air_env...
opening_nor...
produc...
const3
k=AirGap
produc...
gain1
k=-1
pneumatic

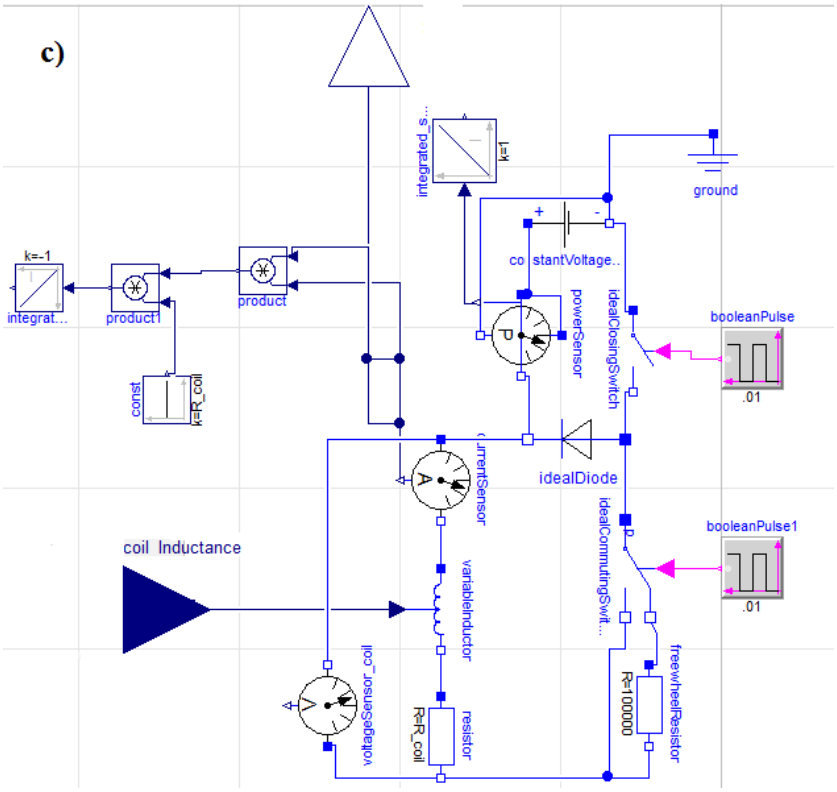

Fig. 6 Dymola model of: (a) pulsed pilot stages; (b) pneumatic domain; (c) electro-magnetic domain

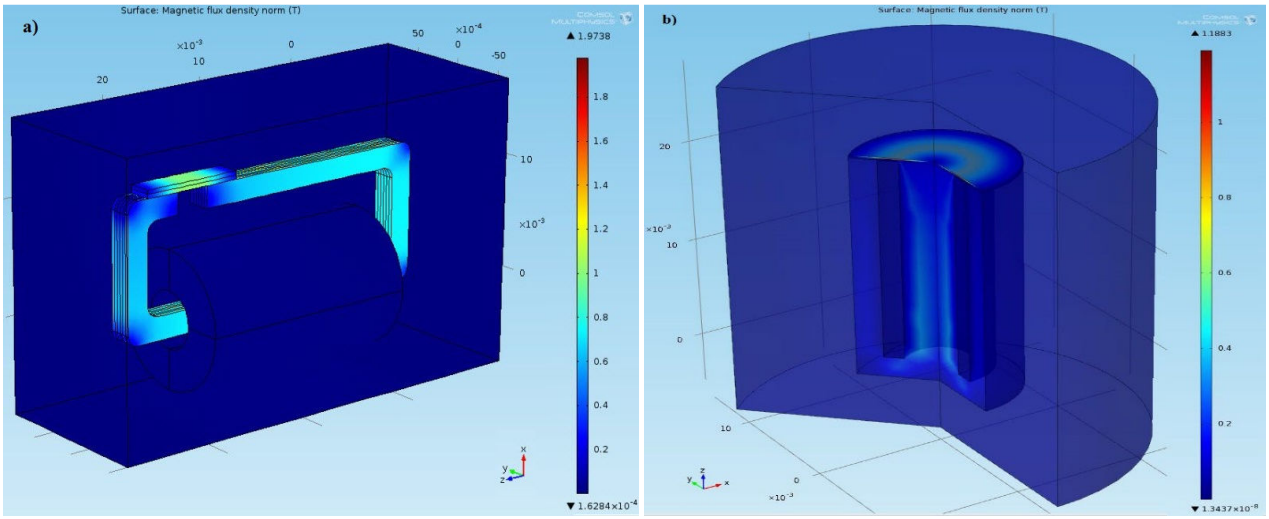

Fig. 7 Magnetic flux density distribution of: (a) pilot 1; (b) pilot 2

TABLE I
POWER CONSUMPTION OF PILOT 1 AND PILOT 2 BASED ON SIMULATION

	Opening Power (mW)	Holding Power (mW)	Total Power (mW)
Pilot 1	4.1	1.9	5.7
Pilot 2	3.29	1.7	4.6

After feeding 3D tables to the system, threshold voltage method is used to obtain minimum current required to actuate pilots. Based on this method, an initial voltage (in this case 2 V) is chosen and then pulse width is minimized to find the minimum current that moves the mass (flapper). Fig. 9 respectively presents the displacement of the flapper (a), energy consumption (b), opening input voltage (c), and holding input voltage of the system (d) of pilot 1 and pilot 2. Once the threshold voltage and minimum current are known, total power of the system is determined according to (4) and (5). Table I demonstrates the total and holding power consumption of each pilot.

B. Experimental Verification

Once simulations show that conceptual designs can fulfill the requirements, they are verified in reality. Hence, prototypes of two conceptual pulsed pilots are manufactured and tested in the required conditions. Different types of experiments were executed on the pilots to understand the dynamic behavior of the multiphysics system. Experimental results of pilot 1 and pilot are presented as follows. Detail of the experiment setup is presented in Appendix.

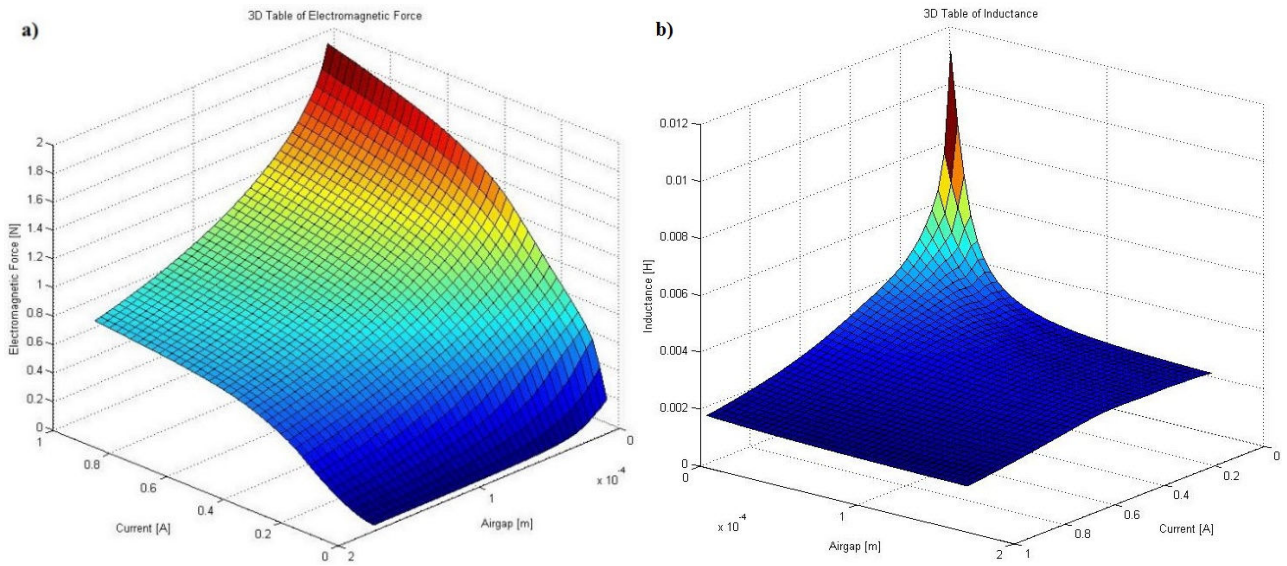

Fig. 8 3D plot of: (a) electromagnetic force, flapper position and current; (b) static inductance, flapper position and current

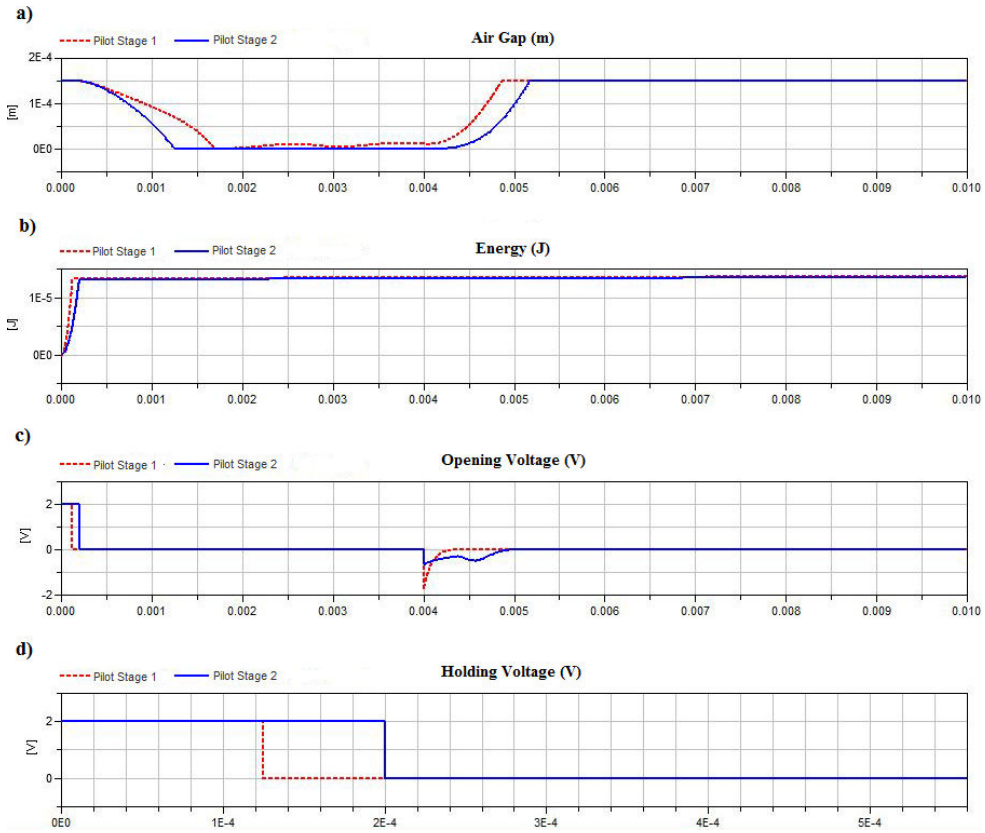

Fig. 9 (a) displacement of the flapper, (b) energy consumption, (c) opening input voltage, (d) holding input voltage of the pilot 1 and pilot 2 concepts

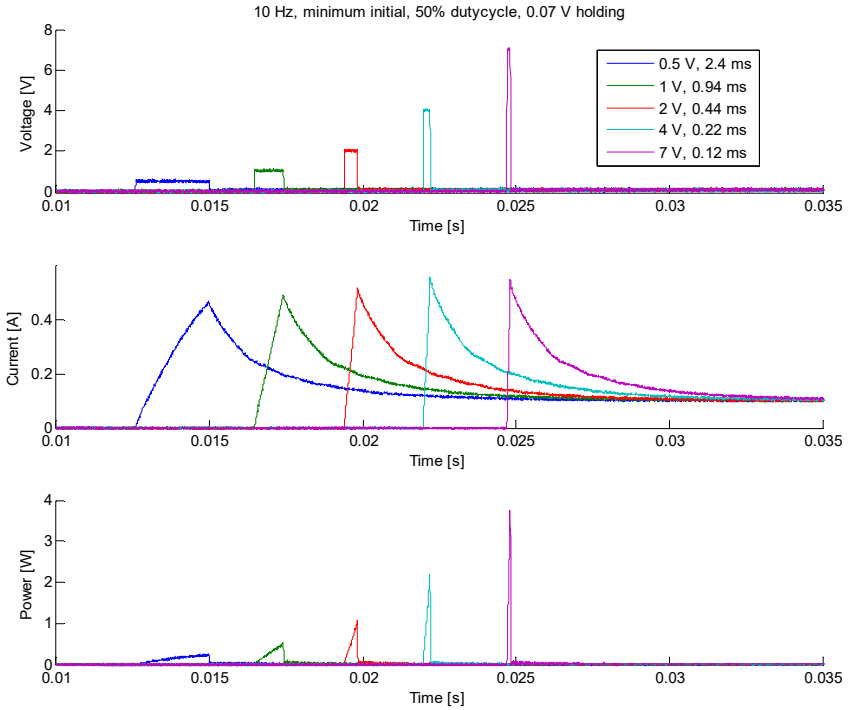

Fig. 10 Voltage, current, and power results of pilot 1 at 100 Hz and 50% duty cycle

1) Pilot 1

When energizing the pilot with a constant voltage, it begins to switch at 0.34 V. The voltage to keep it opened is 0.07 V. At about 0.6 V, the continuous current limit of 3 A of the voltage follower stage is reached. Note that this is a considerably high current which should only be used for very short time periods.

As the driver signal of the pilot has not been optimized for lowest power consumption, with the described two level voltage control, several initial voltages can be set. The results of these settings at a 10 Hz rate are shown in Fig. 10.

With higher voltages supplied, the critical current is reached more quickly which is basically the same in all cases. The power consumption is also comparable for the different cases, see Table II. However, the values above are for a 50% duty cycle. For higher duty cycles the holding voltage will be on for a longer time creating an increased power consumption. The holding voltage is 0.07 V at a current of 0.1 A. This means that the holding current is already over the power target. The relatively positive values shown in Table II are created by the fact that, at 50% duty cycle, the energy consumption is zero during 50% of the time.

TABLE II
POWER CONSUMPTION OF PILOT 1 FOR DIFFERENT DRIVING VOLTAGE LEVELS IN FIG. 10

Voltage (V)	0.5	1	2	4	7
Total Power (mW)	8.5	8.5	8.6	8.9	12.5

2) Pilot 2

In this experiment, the same setup as in the previous section is used. However, initial experiments showed that the voltage control that was used for pilot 1, led to rather high power consumption. The voltage on-time during the opening phase was unnecessarily long. Shortening this time gave unstable performance. Lengthening this time gave rise to high peak currents and power consumption. In this experiment, an extra time period and voltage level is added which starts with a 7-V short pulse to ramp up the current fast and high enough to make the disc flapper move, as illustrated in Fig. 11. Then, a second time period in which the voltage is reduced (3 V), but typically enough to keep the current close to the value at the end of time period 1. Then, the third phase is the holding phase 0.135 V. In this rather long time period, the voltage is reduced to a very low level, just enough to keep the disc on the core. Thus, the total power consumption of this concept reaches 7.6 mW which is just below the limitation. In order to verify the functionality and power consumption, the concept is tested with different duty cycles, as shown in Fig. 11. Results of the power consumption of the pilot 2 in various duty cycles are presented in Table III.

TABLE III
POWER CONSUMPTION OF PILOT 2 FOR DIFFERENT DUTY CYCLES

Duty Cycle (%)	15	37	80	90
Total Power (mW)	7.3	7.4	7.5	7.6

This adaptation was most likely needed due to dynamics of the mechanical system. When impacting on the core the disc has the tendency to rebound. By keeping the current, and thereby the attractive force high for a longer time, the disk is stabilized in the pneumatically open position. The same could

be achieved by only increasing time period 1; however, the current would, in that case, continue to rise, leading to unnecessarily high forces and power consumption.

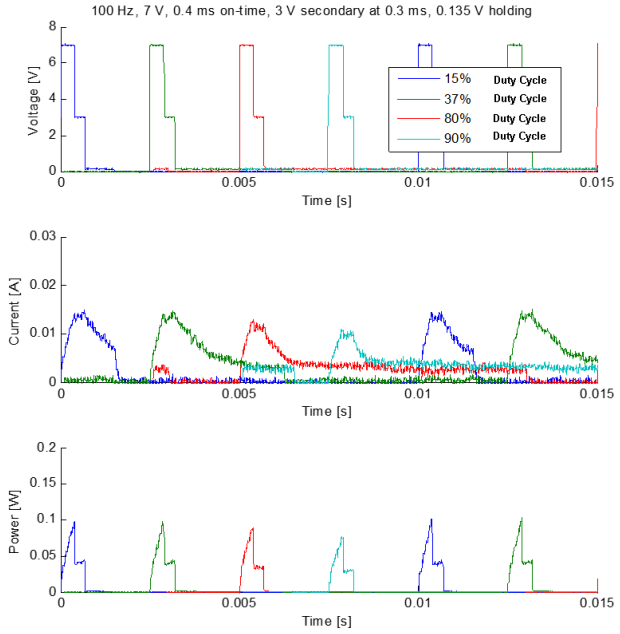

Fig. 11 Voltage, current and power results of pilot 2 at 100 Hz and different duty cycles

V. Discussion and Conclusion

In order to properly compare the dynamic performance of pilot 1 and 2, both concepts are modeled with the same configuration (mechanical and electrical). In this comparison, the power consumption of the concepts is set to be the same. In this condition, pilot 2 has better dynamic performance and faster response than pilot 1, as demonstrated in Fig. 9. Obviously, the major reason is that flapper mass of pilot 1 is much heavier than pilot 2, hence flapper acceleration of pilot 1 is lower than pilot 2. Furthermore, eddy current generated in flapper of pilot 1 hinders the movement of flapper moving away from core, this flapper should be made of laminated ferro-material. Meanwhile, flapper spring of pilot 2 is very thin, hence eddy current effect is negligible. The last reason may possibly be the magnetic flux flow and less magnetic leakage of pilot 2 electro-magnetic actuation mechanism. Furthermore, the pilot 2 concept has easier assembly from production aspect than pilot 1. On the other hand, pilot 2 concept is much larger than pilot 1 due to its axisymmetric design. Advantages and drawbacks of each pilot are summarized in Table IV.

To conclude, in this work, two low power consuming pilot stage concepts are designed to regulate the pressure (10 bar) of a pneumatic mechanism. Both pilot 1 and pilot 2 are derived by pulse width modulation method to reduce the power consumption. Sophisticated dynamic model of each concept is developed, and their feasibility is verified by experimental measurements.

Since the major requirement of this work has been the power consumption of the device, results have shown that only pilot 1 can operate below the required power (8 mW). However, no form of lifetime testing has been performed in this study. Besides, the fatigue properties of the iron-cobalt-chromium soft magnetic alloy used in spring flapper of pilot 2 is unknown to scholars and requires further investigation on lifecycle of this material. Thus, future investigation of life cycle of pilots is essential.

TABLE IV
Advantages and Drawbacks of Pilot 1 and 2

	Advantages	Drawbacks
Pilot 1	• Simple design. • Compact design. • Small moving parts.	• Relatively high power consumption. • Slow response. • Difficult to assembly.
Pilot 2	• Low power consumption. • High performance. • High magnetic efficiency (low loss and low leakage).	• Large dimension design. • Large moving part. • Complex design.

Appendix

This section describes the experiment setup designed in this study, as presented in Fig. 12. The supplied air is first fed through a mass flow meter, then a flow restrictor and the then pilot stage that exhausts to the environment. Between the pilot and the flow restrictor, a high bandwidth pressure sensor is connected. The flow restrictor can be used to create the functionality of a pressure regulator. By using this, a pneumatic resistance bridge is created and by changing the duty cycle of the pilot stage, the pressure in the hose between the regulator and the pilot can be changed.

Instruments used for the experiments are mentioned below:

- LCR meter (Agilent U1733C) is used to measure the properties of the coil.
- Digital oscilloscope (YokogawaDLM2024) is used to record voltage and current signals with high band-width.
- Thermal mass flow meter (Brooks 5860S) is used earlier to determine mass flow of the pilot stage.
- Pressure sensors (Keller PR-23) is used to measure the pressure.
- Current probe is used to measure the electrical current.

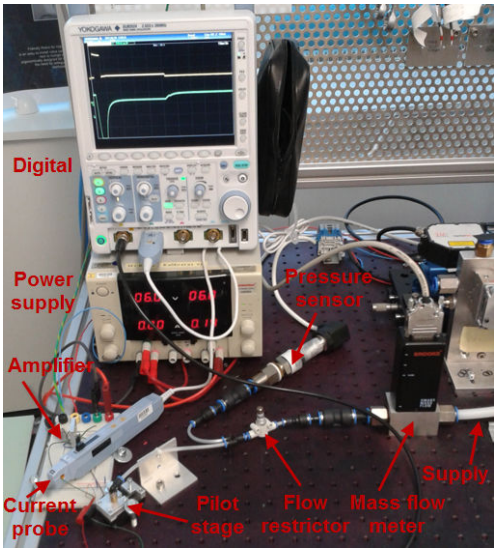

Fig. 12 Conceptual Pilot experiment setup

REFERENCES

[1] K. Kawashima, C. Youn, T. Kagawa, "Development of a nozzle-flapper-type servo valve using a slit structure", J Fluid Eng-T Asme, 2007, vol.129, no.5, pp. 573-578.
[2] C. Garvin, A. Mathew, "The application of the method of simultaneous stabilization to the control of a nonlinear servo valve", IEEE T Contr Syst T, 1996, vol. 4, no.6, pp, 654-664.
[3] X. Pan, G. Wang, Z. Lu. "Flow field simulation and a flow model of servo-valve spool valve orifice", Energ Convers Manage, 2011, vol. 52, no. 10, pp. 3249-3256.
[4] J. Mchenya, S. Zhang, S. Li, "Visualization of Flow-Field between the Flapper and Nozzle in a Hydraulic Servo-valve", Adv Mater Res-Switz, 2012, pp. 402:407.
[5] S. Zhang, H. Xu, S. Li, "A numerical study of flow field in a flapper-nozzle pilot valve under working condition", 2015 International Conference on Fluid Power and Mechatronics (FPM), pp.312-316, 2015.
[6] L. Zhang, J. Luo, R. Yuan, M. He, "The CFD Analysis of Twin Flapper-nozzle Valve in Pure Water Hydraulic", Procedia Engineer, 2012, vol. 31, pp. 220-227.
[7] G. Bao, T Cheng, Y. Huang, X. Guo, H. Gao, "A nozzle flapper electro-pneumatic proportional pressure valve driven by piezoelectric motor", Proceedings of 2011 International Conference on Fluid Power and Mechatronics, pp,191-195, 2011.
[8] J. Wang, G. W. Jewell, and D. Howe, "A general framework for the analysis and design of tubular linear permanent magnet machines," IEEE Trans. Magn., vol. 35, no. 3, pp. 1986–2000, May 1999.
[9] I. J. C. Compter, "Electro-dynamic planar motor," Precis. Eng., vol. 28, pp. 171–180, 2004.
[10] G. Krebs, A. Tounzi, B. Pauwels, D. Willemot, and F. Piriou, "Modeling of a linear and rotary permanent magnet actuator," IEEE Trans. Magn., vol. 44, no. 11, pp. 4357–4360, Nov. 2008.
[11] L. Yan, I. M. Chen, C. K. Lim, G. Yang, W. Lin, and K.-M. Lee, "Design and analysis of a permanent magnet spherical actuator," IEEE/ASME Trans. Mechatronics, vol. 13, no. 2, pp. 842–932, Apr. 2008.
[12] D. K. Abeywardana; A. P. Hu; Z. Salcic; K. I. Wang, "Ultra-low energy bi-state microactuator with wireless power and control capability", 2016 IEEE PELS Workshop on Emerging Technologies: Wireless Power Transfer, pp, 135 – 139, 2016.
[13] S. H. Jeong, S. K. Jong and G. K. Jan, "Structural optimization of a large-displacement electromagnetic Lorentz force microactuator for optical switching applications", J. Micromech. Microeng., vol. 14, pp.1585–1596, 2004.
[14] J. D. Grade, H. Jerman and T. W. Kenny, "Design of large deflection electrostatic actuators", J. Microelectromech. Syst., vol. 8, pp. 2–9, 2003.
[15] J. S. Ko, M. L. Lee, "Development and application of laterally driven electromagnetic microactuator", Appl. Phys. Lett., vol. 81, pp. 547-549, 2002.
[16] "Non-Oriented Electrical Steel." (Online). Available: http://cogent-power.com/products/non-oriented-electrical-steel (Accessed: 20-Jan-2017).
[17] "Dymola." (Online). Available: https://www.3ds.com/products-services/catia/products/dymola/ (Accessed: 23-Mar-2017).
[18] "COMSOL Multiphysics® Modeling Software." (Online). Available: https://www.comsol.com/ (Accessed: 23-Mar-2017).